Power Quality Improvement using Shunt Active Power Filter: An Industrial Zone Case Study

FOUAD ZARO
Electrical Engineering Department,
Palestine Polytechnic University,
Hebron City,
PALESTINE

Abstract: - Power quality (PQ) improvement using active power filters (APF) is a topic of growing interest. APFs are effective in reducing harmonic distortion and improving power factor. They can be used in a variety of applications to improve the performance and reliability of electrical equipment. To address concerns with PQ improvement, this study offers an application of shunt APF in an industrial zone smart grid. the non-linear loads and unpredictable harmonics produced by on-grid PV inverters that represent the architecture of an industrial smart grid. Utilizing the MATLAB/SIMULINK software suite, a detailed design of the APF and associated hysteresis current control technique is provided. The findings demonstrate that APF is a useful tool for reducing total harmonic distortion (THD) and has a quick dynamic reaction to control grid voltage and power factor.

Key-Words: - Shunt active power filter, Harmonics mitigation, Power factor correction, Distributed generation, Hysteresis current controller, Power quality improvement

Received: August 25, 2022. Revised: August 21, 2023. Accepted: September 18, 2023. Published: October 26, 2023.

1 Introduction

Power quality (PQ) concerns are brought on by the integration of utility systems with new renewable energy sources like solar and wind technology. How to raise the standard of electrical services is one of the primary research areas in the field of smart grids. The main cause of poor PQ issues including harmonics, poor power factor, sag, and swell distortions is the continued development of power electronic devices like nonlinear loads, variable frequency drives, and soft starters. Therefore, it's crucial to consider new approaches to raise the caliber of utility services, [1].

One of the most common power quality problems is harmonic distortion. Harmonics are multiples of the fundamental frequency of the power supply (typically 50 or 60 Hz). They can be caused by nonlinear loads, such as computers, power electronics devices, and lighting. Harmonics can cause a number of problems, including: increased heating of electrical equipment, reduced efficiency of electrical equipment, interference with communication and signaling systems, and malfunction of electronic equipment, [2], [3].

The two primary methods for reducing PQ issues are active and passive power filters. Passive power filters (PPF) have several shortcomings compared to active power filters (APF), including the inability to compensate for sub-harmonics, tuning circuit accuracy, and trouble with their enormous size, [4].

In addition to reducing harmonics and raising the power factor to unity, many research subjects in the field of renewable energy technology center on providing real power to the loads. Due to their advantages, such as their quick response to grid fluctuations, capacity to compensate for random harmonics and high control accuracy, APFs have recently emerged as the most efficient method to eliminate harmonics, inter-harmonics, and sub-harmonics, [5], [6]. To cancel a wide range of harmonics that affect the system and raise the grid's power factor (PF) to unity, APFs inject a current into the point of common coupling (PCC) that is equal to but opposite in direction to the grid harmonics. They also generate and absorb reactive power into the grid. Furthermore, APFs keep the grid system balanced and stable with load variations and grid transients, [7], [8].

There are two types of APF, each one has its advantages and disadvantages depending on its effects and capacity: Series active power filter; this filter, which is used in series with the loads, is intended to reduce the grid's voltage harmonics by generating negative voltage harmonics that cancel the effects of the load's voltage harmonics and maintain the grid's voltage in a pure sine shape throughout transient, sag, and swell events. Shunt active power filter; this filter, which is coupled in

parallel with nonlinear loads, is used to inject a negative current harmonic into the grid to lower the utility's current distortion and raise the grid's power factor, [9], [10].

Voltage source inverters (VSI) and current source inverters (CSI) are the two primary types of inverters. When the grid voltage is distorted, the output of the shunt APF is also changed to control the waveform of the grid's voltage and maintain a clean sine wave. The use of VSI connected in parallel with the grid depends on network voltage. CSI was also parallel to the grid but was used to control how much the current waveform was distorted. Since the total harmonic distortion (THD) of the current from industrial areas and renewable energy sources is substantially higher than the THD of the grid's voltage, the typical method for achieving this is VSI with current reference feedback. Figure 1 shows control strategies of VSI that are connected to an 11kV 50Hz network.

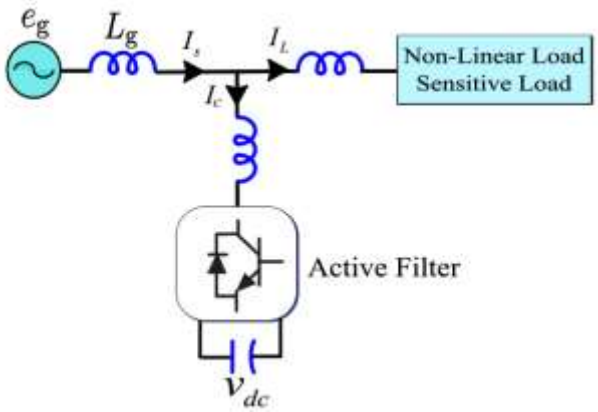

Fig. 1: Control stages of APF connected to grid, [2].

This study represents design shunt APF to solve PQ problems of renewable energy sources that integrate with utility grids to mitigate grid harmonics and improve the PF of the system. A phase VSI inverter consists of six IGBTs with anti-parallel diodes. the output voltage and frequency obtained from the inverter should be in phase, equal, and in the opposite direction of the grid's harmonics to cancel its effects using phase locked loop control circuit (PLL), [10].

2 Problem Formulation

Shunt APF is a three-phase voltage source inverter that is used to reduce random harmonics and correct the power factor (PF) by generating a specified reference current for the IGBT bridge. The three-phase voltages and currents must be measured to determine the reference current, which must then be converted into a two-phase model (direct and quadrature-dq) using the Clark transformation method. After analyzing three-phase reference currents using the inverse Clark transformation, this two-phase reference current is used to gate the inverter bridge, [11], [12], [13]. Figure 2 illustrates the control procedure of reference calculation. Figure 3 shows the overall transfer matrices.

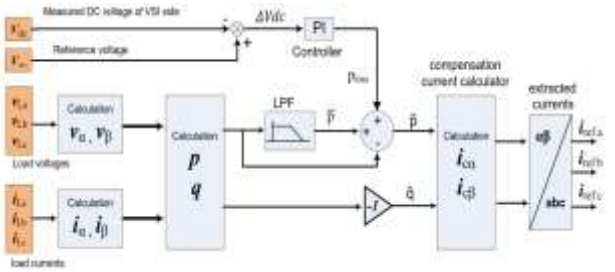

Fig. 2: control procedure of reference current calculation, [11].

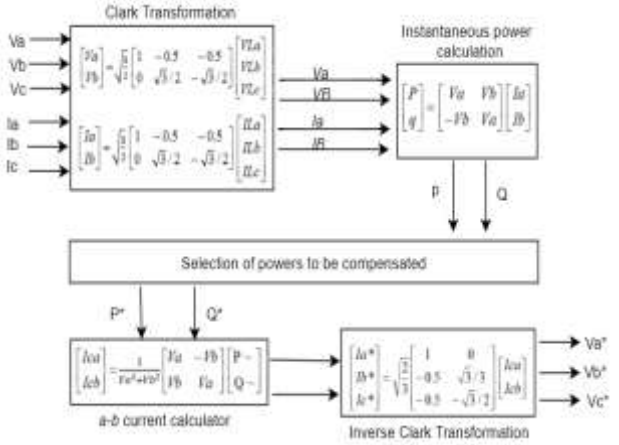

Fig. 3: Overall transfer matrices of generating reference currents, [10].

2.1 Two-phase Calculation

The two-phase calculation method is used to convert three-phase measurements into the two-phase model (direct and quadrature-dq) using the Clark transform to simplify the calculations according to equation (1), [11].

$$\begin{bmatrix} v_\alpha \\ v_\beta \end{bmatrix} = \sqrt{2/3} \begin{bmatrix} 1 & -1/2 & -1/2 \\ 0 & \sqrt{3}/2 & -\sqrt{3}/2 \end{bmatrix} \begin{bmatrix} v_{La} \\ v_{Lb} \\ v_{Lc} \end{bmatrix}$$

$$\begin{bmatrix} i_\alpha \\ i_\beta \end{bmatrix} = \sqrt{2/3} \begin{bmatrix} 1 & -1/2 & -1/2 \\ 0 & \sqrt{3}/2 & -\sqrt{3}/2 \end{bmatrix} \begin{bmatrix} i_{La} \\ i_{Lb} \\ i_{Lc} \end{bmatrix} \quad (1)$$

2.2 Instantaneous Power Calculation

Instantaneous real power (P) and instantaneous reactive power (Q), both include two components,

DC components due to the fundamental of the load current and an AC component corresponding to the harmonic current of the load. This instant power can be calculated depending on equation (2).

$$\begin{bmatrix} p \\ q \end{bmatrix} = \begin{bmatrix} v_\alpha & v_\beta \\ -v_\beta & v_\alpha \end{bmatrix} \begin{bmatrix} i_\alpha \\ i_\beta \end{bmatrix} = \begin{bmatrix} p^- & p^\sim \\ q^- & q^\sim \end{bmatrix} \quad (2)$$

Where $P = P^- + P^\sim$ and $Q = Q^- + Q^\sim$

2.3 AC Real Power Calculation

AC real power reference $P^\sim$ can be extracted from total power P by a low pass filter to separate the two components from each other and select the AC component only. For a given complex power set-point $S_{ref} = P_{ref} + j\, Q_{ref}$ and an output voltage of $V_o = V_{od} + j\, V_{oq}$, Thus, the reference current signals $I_{d\text{-}ref}$ and $I_{q\text{-}ref}$ can be calculated according to equation (3).

$$\begin{bmatrix} i_d^* \\ d_q^* \end{bmatrix} = \frac{1}{v_{od}^2 + v_{oq}^2} \begin{bmatrix} v_{od} & v_{oq} \\ v_{oq} & -v_{od} \end{bmatrix} \begin{bmatrix} P_{ref} \\ Q_{ref} \end{bmatrix} \quad (3)$$

Where P_{ref} and Q_{ref} are reference active and reactive power signals.

2.4 Reference Current Calculation in Two-Phase Mode

The compensating currents $I_{d\text{-}ref}$ and $I_{q\text{-}ref}$ in two-phase mode can calculated depending on equation (4).

$$\begin{bmatrix} i_{c\alpha} \\ i_{c\beta} \end{bmatrix} = \frac{1}{v_\alpha^2 + v_\beta^2} \begin{bmatrix} v_\alpha & -v_\beta \\ v_\beta & v_\alpha \end{bmatrix} \begin{bmatrix} P_{ref} \\ Q_{ref} \end{bmatrix} \quad (4)$$

2.5 Three-phase Reference Current Calculation

Compensating current in three-phase mode can be evaluated depending on two-phase results using inverse Clark transform according to equation (5).

$$\begin{bmatrix} i_{ref\ a} \\ i_{ref\ b} \\ i_{ref\ c} \end{bmatrix} = \sqrt{2/3} \begin{bmatrix} 1 & 0 \\ -1/2 & \sqrt{3}/2 \\ -1/2 & -\sqrt{3}/2 \end{bmatrix} \begin{bmatrix} i_{c\alpha} \\ i_{c\beta} \end{bmatrix} \quad (5)$$

To achieve high output current quality, low-pass filtering of the signal is generated by subtracting the grid-side current Ig from the reference current I_{ref} as shown in Figure 4.

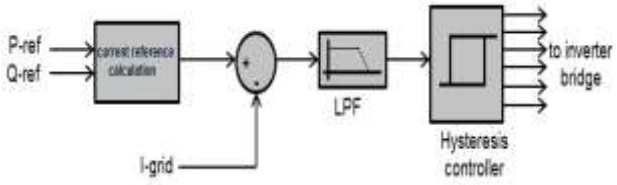

Fig. 4: power controller block diagram

2.6 Hysteresis Band Current Controller

It is a controller used to force the compensated current (If) to follow the calculated reference current (I-ref). The accuracy of the hysteresis controller depends on its hysteresis band (HB) to reduce error value. Figure 5 shows the block diagram of the hysteresis current controller It is a controller used to force the compensated current (If) to follow the calculated reference current (I-ref). The accuracy of the hysteresis controller depends on its hysteresis band (HB) to reduce error value. Figure 5 shows the block diagram of the hysteresis current controller, [11].

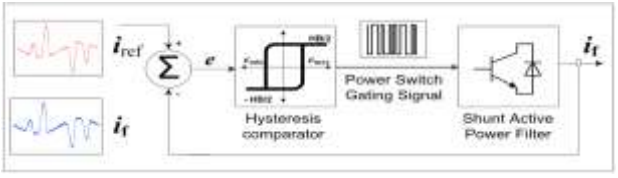

Fig. 5: Block diagram of hysteresis current controller.

3 Simulation Results and Discussions

To study the performance of the photovoltaic on a grid system in the presence of local non-linear load in an industrial zone with the proposed APF connected in parallel with the network. The overall simulation time is 100 ms, and shunt APF becomes in service after the first two cycles (40 ms), the simulation was done using MATLAB/ SIMULINK and carried out as follows.

3.1 Overall System Description

Shunt APF is connected to an 11 kV, 50 Hz grid, to compensate and mitigate the effect of non-linear load that represents the topology of industrial zone loads. Figure 6 shows the overall system design

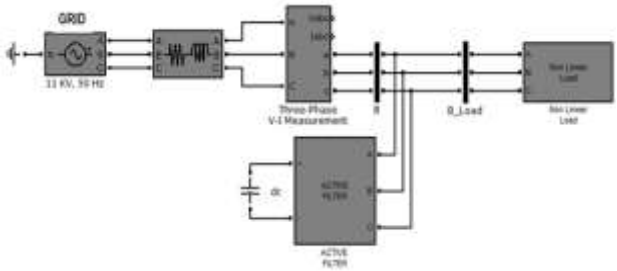

Fig. 6: Overall system design.

3.2 Non-linear Load

The topology of the industrial zone loads are non-linear loads that are full of random harmonics especially the 3rd harmonic, to simulate this topology, a phase AC-DC converter load with 10MW, 26% THD is chosen. Figure 7 shows the load current wave shape.

Fig. 7: Selected three-phase AC-DC converter with its distorted current.

3.3 Two-phase and Instantaneous Power Calculation

The two-phase calculation is done depending on the Clark transform, followed by instantaneous real and reactive power calculation according to equation (2). Figure 8 and Figure 9 show the block diagram and curves of instantaneous power respectively.

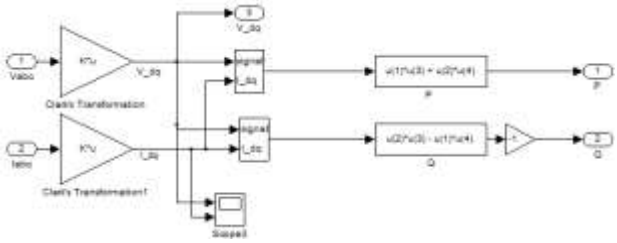

Fig. 8: Two-phase calculation block diagrams followed by an instantaneous power calculation.

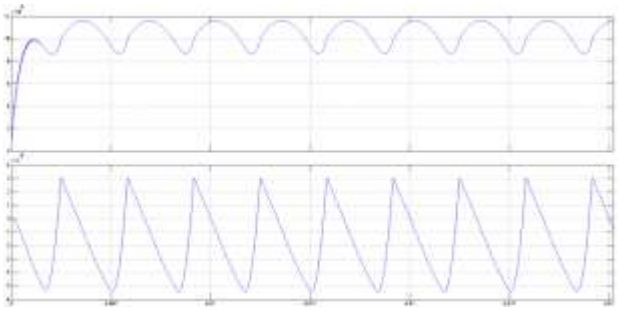

Fig. 9: Instantaneous real and reactive power curves.

3.4 AC Real Power Calculation

Real power (P) out of the previous step consists of two components, P-ac and P-dc components, applying LPF can separate the P-ac and P-dc components from each other. P-ac is also depending on the voltage level across the capacitor at the input of the inverter bridge, it is critical to keep the voltage level stable on a pre-determined value by applying a PI controller, [14], [15]. Figure 10 shows the block diagram of evaluating P-ac. Figure 11 shows the P-ac and P-dc curves respectively.

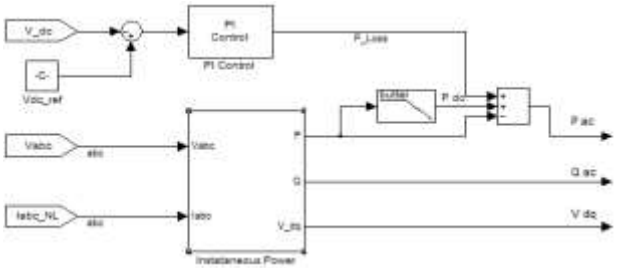

Fig. 10: The block diagram of evaluating P-ac

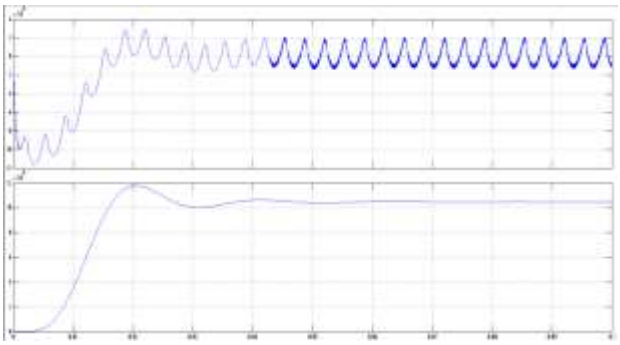

Fig. 11: AC and DC components of real power curves.

3.5 Three-phase Reference Current Calculation

Compensating currents are reference currents of the inverter's performance to mitigate random harmonics and increase the grid's PF up to unity. Generating reference current process depends on evaluating reference currents in a two-phase model according to equation (4) followed by inverse clack

transform to get the references in a three-phase model. Figure 12 shows a block diagram of the phase reference current calculation.

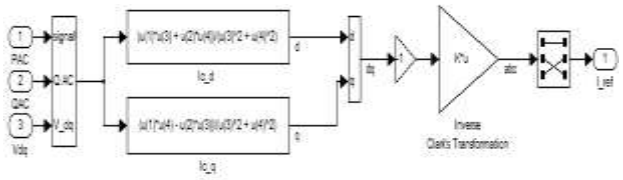

Fig. 12: The block diagram of three-phase reference current calculation.

Note that the summation of references at any instant of time equals zero to make the system stable and balanced. Figure 13 shows reference current curves in the phase and three-phase models respectively.

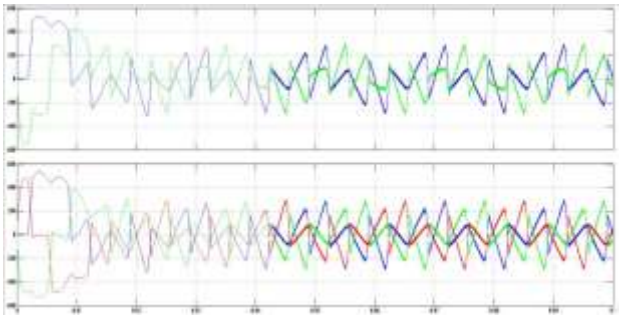

Fig. 13: Reference current curves in two phases and three-phase models respectively.

3.6 Hysteresis Current Controller Design

The compensating current in Figure 13 is an analog signal and is not able to be used as a firing signal of the inverter bridge. The hysteresis controller is used to convert analog signals into digital pulses that are used to fire IGBT gates. Figure 14 shows the block diagram of the hysteresis current controller.

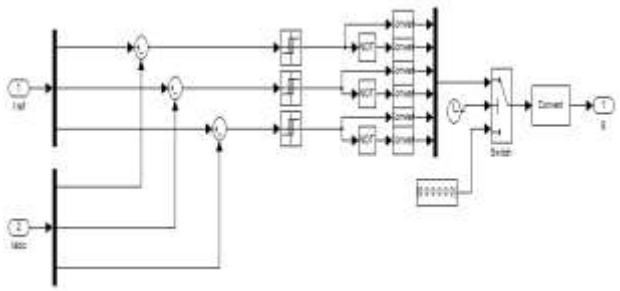

Fig. 14: Hysteresis Current Controller block diagram.

The Hysteresis Controller makes the grid current follow reference currents with a small hysteresis band (HB) to minimize the error value and increase the accuracy of the output current. Figure 15 shows the input and output signal of the Hysteresis Controller with HB = 0.02.

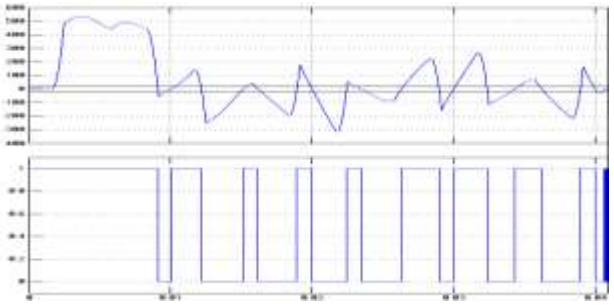

Fig. 15: Input and output signal of hysteresis controller with HB = 0.02.

4 Simulation Results Discussion

APF is connected in parallel to the industrial zone grid to mitigate a wide range of harmonics and keep the output voltage and current pure sine wave, low THD, stable with load variations. Figure 16 shows the current wave shapes before and after installing APF.

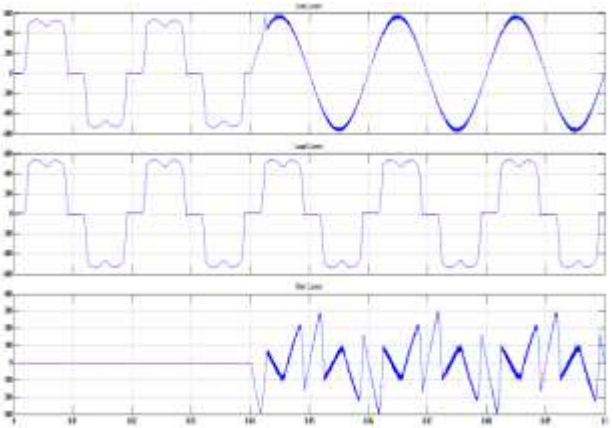

Fig. 16: Current wave shapes before and after installing APF. (a) grid current, (b) load current, (c) filter current.

The SAPF was installed at the point of common coupling (PCC) between the industry's power supply and its nonlinear loads. The SAPF was rated at 500 kVA and was designed to compensate for harmonic currents up to the 50^{th} order. Table 1 shows the THD of voltage and current and PF measurements before and after the installation of the SAPF.

The installation of the SAPF resulted in a significant improvement in the power quality at the load. The THD of voltage and current was reduced significantly, and the power factor was improved. The energy consumption of the industry was also reduced by 5%.

Table 1. The power quality measurements before and after the installation of the SAPF

Parameter	Before SAPF	After SAPF
THD of Voltage	5.5 %	1.5 %
THD of Current	25 %	4 %
Power Factor	0.8	0.96

4 Conclusion

This study used a hysteresis current controller constructed by the MATLAB/SIMULINK software to analyze the performance of SAPF in a real industrial zone with a non-linear load that is full of harmonics for PQ enhancement. The results of the proposed SAPF's design using instantaneous reactive power theory (p-q theory) show that adding SAPF can significantly enhance the performance of the smart grid.

SAPFs are a valuable tool for improving power quality. They are effective in reducing harmonic distortion and improving power factor. SAPFs can be used in a variety of applications to improve the performance and reliability of electrical equipment. With the suggested method, harmonics in the source current and load voltage under nonlinear load are successfully compensated. The outcomes of the simulation demonstrate that the THD complies with IEEE standard 519, i. e. that is, less than 5%. The suggested strategy performs well in the system under various load variations.

To further enhance power quality and efficiency, the manufacturing plant may consider implementing additional technologies such as voltage regulators and energy management systems. Additionally, continuous monitoring and periodic maintenance of the SAPF are crucial for long-term success.

In future work, the author suggests designing and developing a parallel-serial topology (Unified Power Quality Conditioner (UPQC)) given the many benefits they offer, such as voltage and current harmonics filtering.

References:

[1] Subhashree Choudhury, George Tom Varghese, Satyajit Mohanty, Venkata Ratnam Kolluru, Mohit Bajaj, Vojtech Blazek, Lukas Prokop, Stanislav Misak, Energy management and power quality improvement of microgrid system through modified water wave optimization, *Energy Reports*, Vol. 9, 2023, pp. 6020-6041.

[2] Razmi Darioush, Tianguang Lu, Behnaz Papari, Ehsan Akbari, Gholamreza Fathi, and Mojtaba Ghadamyari, An Overview on Power Quality Issues and Control Strategies for distribution networks with the presence of distributed generation resources (DGs), *IEEE Access*, Vol. 11, 2023, pp.10308-10325.

[3] Fouad Zaro, Power Quality Disturbances Detection and Classification Rule-Based Decision Tree, *WSEAS Transactions on Signal Processing*, Vol. 17, 2021, pp. 22-27. https://doi.org/10.37394/232014.2021.17.3

[4] R. N. Beres, X. Wang, M. Liserre, F. Blaabjerg and C. L. Bak, A review of passive power filters for three-phase grid-connected voltage-source converters, *IEEE Journal of Emerging and Selected Topics in Power Electronics*, Vol.4, No.1, 2016, pp. 54-69.

[5] Salah Alqam, Fouad Zaro, Power Quality Detection and Classification Using S-Transform and Rule-Based Decision Tree, *International Journal of Electrical and Electronic Engineering & Telecommunications*, Vol. 8, No. 1, 2019, pp. 45-50.

[6] M. Alhasheem, P. Mattavelli, and P. Davari, Harmonics mitigation and non-ideal voltage compensation utilizing active power filter based on predictive current control, *IET Power Electron.*, Vol. 13, No. 13, 2020, pp. 2782–2793.

[7] Takagi, Kazuto, and Hideaki Fujita, A three-phase grid-connected inverter equipped with a shunt instantaneous reactive power compensator, *IEEE Transactions on Industry Applications*, Vol. 55, No. 4, 2019, pp. 3955-3966.

[8] S. R. Das, P. K. Ray, A. K. Sahoo, S. Ramasubbareddy, T. S. Babu, N. M. Kumar, R. M. Elavarasan, and L. Mihet-Popa, ‘‘A comprehensive survey on different control strategies and applications of active power filters for power quality improvement,’’ *Energies*, Vol. 14, No. 15, 2021, pp. 4589-4598.

[9] Toumi, Toufik, Ahmed Allali, Abdelmalek Meftouhi, Othmane Abdelkhalek, Abdallah Benabdelkader, and Mouloud Denai, Robust control of series active power filters for power quality enhancement in distribution grids: Simulation and experimental validation, *ISA transactions*, Vol.107, 2020, pp. 350-359.

[10] Roselyn, Dr J. Preetha, Devraj Sen, Pratyaksha Lal, Nayanika Purkayastha Purkayastha, and C. Nithya, Development of

hysteresis current controller for power quality enhancement in grid connected PV system, *International Journal of Electrical Engineering and Technology*, Vol. 11, No. 4, 2020, pp. 8-21.

[11] Moftah, Mohamed Amin, Gaber El-Saady, and El-Noby A. Ibrahim. "Active power filter for power quality enhancement of photovoltaic renewable energy systems." *Smart Grid (SASG), 2016 Saudi Arabia. IEEE*, 2016.

[12] L. Polleux, G. Guerassimoff, J.-P. Marmorat, J. Sandoval-Moreno, and T. Schuhler, ‘‘An overview of the challenges of solar power integration in isolated industrial microgrids with reliability constraints,’’ *Renew. Sustain. Energy Rev.*, vol. 155, Mar. 2022, Art. no. 111955.

[13] Boopathi, Rajendran, and Vairavasundaram Indragandhi, Control techniques for renewable energy integration with shunt active filter: a review, *International Journal of Ambient Energy*, Vol. 44, No. 1, 2023, pp. 424-441.

[14] S. Hoseinnia, M. Akhbari, M. Hamzeh, and J. M. Guerrero, A control scheme for voltage unbalance compensation in an islanded microgrid, *Electr. Power Syst. Res.*, Vol. 177, 2019, Art. no. 106016.

[15] R. Selvaganapathy, R. Kannan, and A. Ravi, Allocation of facts devices for power quality improvement, *Int. J. Elect. Eng. Technol.*, Vol. 12, No. 1, 2021, pp. 154-162.

Contribution of Individual Authors to the Creation of a Scientific Article (Ghostwriting Policy)

The author contributed to the present research, at all stages from the formulation of the problem to the final findings and solution.

Sources of Funding for Research Presented in a Scientific Article or Scientific Article Itself

No funding was received for conducting this study.

Conflict of Interest

The author has no conflicts of interest to declare.

Creative Commons Attribution License 4.0 (Attribution 4.0 International, CC BY 4.0)

This article is published under the terms of the Creative Commons Attribution License 4.0
https://creativecommons.org/licenses/by/4.0/deed.en_US